European Journal of Human Genetics (2008) 16, 462–470

www.nature.com/ejhg

ARTICLE

Mild functional effects of a novel *GFAP* mutant allele identified in a familial case of adult-onset Alexander disease

Tiziana Bachetti[1], Francesco Caroli[1], Paola Bocca[2], Ignazia Prigione[2], Pietro Balbi[3], Roberta Biancheri[4], Mirella Filocamo[5], Caterina Mariotti[6], Davide Pareyson[6], Roberto Ravazzolo[1,7] and Isabella Ceccherini*[,1]

[1]*Laboratory of Molecular Genetics, G Gaslini Institute, Genoa, Italy;* [2]*Laboratory of Oncology, G Gaslini Institute, Genoa, Italy;* [3]*Service of Neurophysiopathology, S Maugeri Foundation, Montescano, Italy;* [4]*Muscular and Neurodegenerative Disease Unit, G Gaslini Institute, Genoa, Italy;* [5]*'Diagnosi Pre-Postnatale Malattie Metaboliche' Laboratory, G Gaslini Institute, Genoa, Italy;* [6]*Division of Biochemistry and Genetics, 'C Besta' Neurological Institute, Milan, Italy;* [7]*Department of Pediatrics and CEBR, University of Genoa, Genoa, Italy*

Alexander disease is a neurological genetic disorder characterized by progressive white-matter degeneration, with astrocytes containing cytoplasmic aggregates, called Rosenthal fibers, including the intermediate filament glial fibrillary acidic protein (GFAP). The age of onset of the disease defines three different forms, infantile, juvenile and adult, all due to heterozygous *GFAP* mutations and characterized by a progressive less severe phenotype from infantile to adult forms. In an Italian family with a recurrent mild adult onset of Alexander disease, we have identified two GFAP mutations, coupled on a same allele, leading to p.[R330G; E332K]. Functional studies on this complex allele revealed less severe aggregation patterns compared to those observed with p.R239C *GFAP* mutant, associated with a severe Alexander disease phenotype. Moreover, in addition to confirming the involvement of the ubiquitin–proteasome system in cleaning cells from aggregates and a dominant effect of the novel mutant protein, in cells expressing the mild p.[R330G; E332K] mutant we have observed that indirect αB-crystallin overexpression, induced by high extracellular potassium concentration, could completely rescue the correct filament organization while, under the same experimental conditions, in cells expressing the severe p.R239C mutant only a partial rescue effect could be achieved.
European Journal of Human Genetics (2008) **16,** 462–470; doi:10.1038/sj.ejhg.5201995; published online 16 January 2008

Keywords: GFAP mutation; adult-onset Alexander disease; aggregates; αB-crystallin

Introduction

Alexander disease is a progressive rare and usually fatal devastating disorder of the central nervous system[1] characterized by demyelination of the white matter[2] and by the presence of Rosenthal fibers, containing glial fibrillary acidic protein (GFAP), αB-crystallin and heat-shock protein 27.[3] Alexander disease manifests with different clinical and pathological signs, mainly depending on the age of onset of the disease. In particular, infantile, juvenile and adult forms can be distinguished on the basis of increasing age of onset, which correlates with progressively less severe phenotypes of the disease.[4] While the infantile form is characterized by motor and mental retardation, bulbar dysfunction, seizures and megalencephaly

*Correspondence: Dr I Ceccherini, Laboratorio di Genetica Molecolare, Istituto Giannina Gaslini, L.go Gerolamo Gaslini 5, I-16148 Genova, Italy. Tel: +39 010 5636800; Fax: +39 010 3779797;
E-mail: isa.c@unige.it
Received 29 May 2007; revised 21 November 2007; accepted 28 November 2007; published online 16 January 2008

due to a marked defect in myelination in the frontal lobes, juvenile and adult forms show difficulties of coordination, speech and swallowing without myelin and mental function defects.[4] The three forms, although characterized by a wide phenotypic heterogeneity, are all associated with heterozygous amino-acid changes in the *GFAP* gene, encoding the homonymous astrocyte-specific protein belonging to the type III intermediate filament (IF) family.[5]

Although the vast majority of nucleotide changes seems clustered in specific codons of exons 1, 4, and 8,[6] protein domains 1A, 1B, 2A and 2B, characterized by α-helical structures, are frequently defective.

Functional studies have shown cytoplasmic inclusions similar to Rosenthal fibers in murine astrocytes and in several cell lines overexpressing wild-type (wt) *GFAP*, suggesting that formation of GFAP aggregates could be due to elevated production of the protein.[7,8] More recently, studies have been focused on the effect induced by the most frequent mutations, associated with the severe infantile phenotype, p.R239C and p.R239H. In particular, it has been shown that the p.R239C substitution can prevent formation of a regular filamentous pattern, alter the normal solubility of the protein in several cell lines and impair the wt GFAP organization.[9–11] Moreover, as the accumulation of p.R239C GFAP seems to lead to a decrease of proteasome activity, this latter proteasomal hypofunction likely cooperates to produce further GFAP accumulation and cellular stress responses, thus inducing a continuous raising in the aggregation rate.[11] Finally, a more recent work has provided evidence for a link between the extent of GFAP functional alteration and the domain where mutations are located.[12]

In this paper, we report the first functional study aimed at clarifying the effects of the novel c.[988C>G; 994G>A] complex allele, leading to p.[R330G; E332K], detected in four members of a family affected with adult-onset Alexander disease. In particular, we suggest that the observed differences between effects due to the p.[R330G; E332K] and p.R239C mutations, in terms of both severity of GFAP aggregation rate and rescue of the correct filament organization consequent to indirect αB-crystallin overexpression, account for the different clinical severity of the two associated Alexander forms.

Materials and methods

Family

Clinical and radiological features of four members of a family carrying the novel c.[988C>G; 994G>A] complex allele, leading to p.[R330G; E332K], and affected with adult-onset Alexander disease, have already been reported.[13] Blood samples of the proband (onset: 56 years) and the other members were obtained with informed consent. Genomic DNA was extracted using standard procedures.

GFAP expression plasmid construction

Human wt GFAP-GFP expression construct Total RNA was extracted from U251-MG human astrocytoma cell line (RNeasy Mini Kit, Qiagen). GFAP cDNA (GeneBank accession no. S40719) lacking the stop codon was prepared from 1 μg of total RNA (Advantage RT-for-PCR kit) and amplified with the forward primer, containing the underlined *Eco*RI cleavage site, GFAP–*Eco*RI(F) 5′-AAATGAATTCGAGCCA GAGCAGGATGGAG-3′ and the reverse primer, containing the underlined *Sac*II cleavage site, GFAP–*Sac*II(R) 5′-CA ACCCGCGGCATCACATCCTTGTGCTCCTG-3′. The PCR product was cloned upstream of the GFP cDNA in the pcDNA3.1/CT-GFP-TOPO vector (Invitrogen), thus allowing for a wt GFAP-GFP fusion product characterized by the 3′ end of the GFAP protein in frame with the 5′ end of the GFP protein. Such a hybrid construct was completely sequenced using a Big Dye Terminator cycle sequencing kit (Applied Biosystem) on an ABI 3100 DNA automated Sequencer.

Mutated GFAP-GFP expression constructs GFAP missense mutations were generated through site-specific mutagenesis using the wt cDNA plasmid as a template. In particular, primers GFAP–*Eco*RI(F) + GFAP(R239C)R (5′-CC TCATACTGCGTGCAGATC-3′) and primers GFAP(R239C)F (5′-GATCTGCACGCAGTATGAGG-3′) + GFAP–*Sac*II(R) were used for p.R239C-GFP; primers GFAP–*Eco*RI(F) + GFAP (R330G)R (5′-CTTCCTCCAGCCCCGCC-3′) and GFAP (R330G)F (5′-GGCGGGGCTGGAGGAAG-3′) + GFAP–*Sac*II(R) were used for p.R330G-GFP; primers GFAP–*Eco*RI(F) + GFAP(E332K)R (5′-CTTCCTTCAGCCGCGCC-3′) and GFAP (E332K)F (5′-GGCGCGGCTGAAGGAAG-3′) + GFAP–*Sac*II(R) were used for p.E332K-GFP; primers GFAP–*Eco*RI(F) + GFAP(R330G-E332K)R (5′-CTTCCTTCAGCCCCGCC-3′) and primers GFAP(R330G-E332K)F (5′-GGCGGGGGCTGAA GGAAG–3′) + GFAP–*Sac*II(R) were used for p.[R330G; E332K]-GFP. All PCR products were completely sequenced with both plasmid- and GFAP-specific primers.

Far-red fluorescence wt GFAP The fragment containing the wt GFAP cDNA was *Eco*RI–*Sac*II double digested from the pcDNA3.1/CT-GFP-TOPO[wild-type GFAP] construct and inserted upstream the HcRed cDNA into the pHcRed1-N1 vector (Clontech) after *Eco*RI–*Sac*II digestion.

Cell culture and transient transfections

U251-MG human astrocytoma cell line was grown in RPMI medium (Euroclone) supplemented with 10% FBS (New Zealand), 1% L-glutamine (100 ×), 100 U/ml penicillin and 100 μg/ml streptomycin in a humidified atmosphere with 5% CO_2. Transient transfections were performed plating 2×10^5 U251-MG cells directly with the transfection mix and adding 1 μg of expression constructs and 3 μl of Lipofectamine 2000 (Invitrogen). To assay dominant-negative effects, 1 μg pHcRed1-N1 GFAP construct was

mixed with increasing amounts of mutated GFAP-GFP expression constructs and 3 μl of Lipofectamine 2000 (Invitrogen). Forty-eight hours after transfection, cells were washed with PBS; after nuclei staining with DAPI (0.2 mg/ml), cell plates were analyzed with a Zeiss Axiophot fluorescence microscope. For each experiment, performed in triplicate, at least 100 cells/plate were analyzed.

Analysis of GFAP protein levels

Transient transfections were performed plating, directly in 60 mm diameter dishes, 3×10^5 U251-MG cells with the transfection mix containing 2 μg of either GFAP wt-GFP, p.[R330G; E332K]-GFP or p.R239C-GFP expression constructs with 6 μl of Lipofectamine 2000 (Invitrogen); 48 h later, the mean fluorescence intensity of an identical amount of cells expressing the different mutant proteins was measured by FACS analysis (FACSCalibur, BD Biosciences, Cell Quest software).

Immunocytochemistry

Forty-eight hours after transfection with the GFP-fused expression constructs, U251-MG cells were prepared as already described.[14] Plates were then incubated with a TRITC-conjugated vimentin- or ubiquitin-specific antibody (Santa Cruz Biotechnology) for 60–90 min and, after washing with PBS, were analyzed with a Zeiss Axiophot fluorescence microscope.

Analysis of *αB-crystallin* expression

U251-MG cells were plated in 60 mm dishes and, after 24 h, added with 10 or 60 mM potassium chloride (KCl).[15] Forty-eight hours later, total RNA was extracted (RNeasy Mini kit, Qiagen) and cDNA (GeneBank accession no. NM_001885) was reverse transcribed from 1 μg of total RNA (Advantage RT-for-PCR Kit, Clontech). A 545 bp fragment containing the full-length *αB-crystallin* coding region was amplified with the forward primer αB-cryst(F) 5′-AATTAAGCTTATG GACATCGCCATCCACCAC-3′ and the reverse primer αB-cryst(R) 5′-AATTGGTACCTTTCTTGGGGGCTGCGGTGA-3′. In addition, evaluation of the housekeeping gene *G3PDH* was performed in the same samples, by using oligonucleotides provided in the Advantage RT-for-PCR Kit and following manufacturer's instruction.

Results

Genetic and clinical features of a family with recurrent adult-onset Alexander disease

In four different members of an Italian family, characterized by recurrent adult-onset Alexander disease, we have identified two novel missense mutations c.988C>G and c.994G>A on a same *GFAP* allele, leading to substitutions p.R330G and p.E332K, respectively. Both mutations were present in the proband (onset: 56 years), in his son (onset: 28 years), and in his two sisters (onset: 53 years; presymptomatic)[13] (Figure 1a). Whereas pseudo-bulbar signs were present in all symptomatic members, the youngest patient had developed neither spasticity nor ataxia, yet.

In vitro organization of GFAP filaments

Altered solubility and disrupted conformation, due to a break in the α-helix stretch, could be predicted for the p.[R330G; E332K] allele by using the SCRATCH software (http://www.ics.uci.edu/~baldig/scratch/index.html)[16] (data not shown). Therefore, as a first experimental step, we have attempted to determine whether prediction of incorrect folding of the GFAP protein carrying the p.[R330G; E332K] allele could be confirmed by the localization and polymerization analysis of the mutant protein.

Expression constructs for the wt GFP-fused GFAP protein, the p.[R330G; E332K] mutant and the p.R239C mutant (this latter already observed to produce an irregular filament pattern in several cell line)[10,11] were transfected in U251-MG human astrocytoma cells. Forty-eight hours later, fluorescence microscope analysis revealed three different GFAP filaments organization patterns: (i) diffused filament assembly (F), (ii) small or large cytoplasmic aggregates on a filamentous pattern (F + A), (iii) cytoplasmic aggregates without a regular filamentous structure (A) (Figure 1b). In particular, in agreement with previous observations,[8] 62% of the U251-MG cells expressing the wild-type protein showed an exclusively filamentous organization of the GFAP filaments. Moreover, as already reported,[10,17] most cells expressing the p.R239C protein showed punctate aggregates, confirming the severe effects of this mutant and that our cellular system was suitable to analyze the pathogenic effect of our novel GFAP mutation. Compared to the wild-type and p.R239C proteins, the construct carrying the complex mutation p.[R330G; E332K]-GFP produced GFAP patterns characterized by intermediate severity; in particular, less than 40% of the cells showed the regular filamentous organization and about half of the cells presented a mixed pattern, including coexistence of aggregates on a relaxed filamentous structure and cells characterized by a GFAP packaged organization (Figure 1c). In addition, transfection of constructs encoding for the single mutant alleles has revealed that, in agreement with *in silico* analysis, the p.R330G and p.E332K changes did not separately induce a cellular phenotype more severe than the p.[R330G; E332K] complex mutation.

In particular, the proportion of cells with a filamentous organization induced by the p.R330G construct was not significantly different from that observed in cells transfected with the wt GFAP, suggesting that the p.R330G change alone does not have any significant effect. On the other hand, p.E332K induced an uncorrected GFAP pattern in a fraction of cells not statistically different from that expressing the complex allele, thus suggesting that the

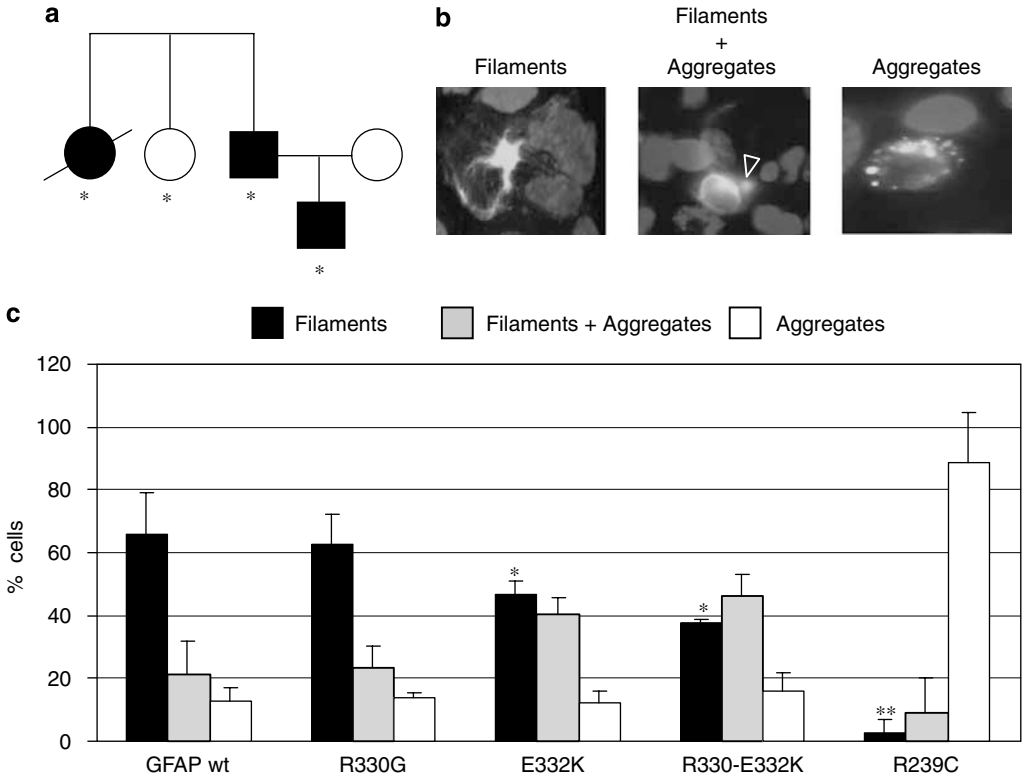

Figure 1 Segregation of the complex allele under analysis and its cellular and molecular effects. (**a**) Members carrying the p.[R330G; E332K] allele are indicated by an asterisk. (**b**) Fluorescence microscopy images showing three different GFAP patterns (filaments only, filaments and aggregates and aggregates only) induced by the p.[R330G; E332K]-GFP protein in U251-MG cells. An aggregate is indicated by the arrow in the middle figure. (**c**) Diagram representation of the percentage of cells expressing different GFAP-GFP mutant constructs, characterized by the three different GFAP patterns. Values are the mean ± SD of three independent experiments performed in duplicate. One-way analysis of variance, performed on the proportions of the filamentous pattern among the five groups, resulted highly significant ($P<0.005$) and prompted us to pair-wise comparisons using the Student's *t*-test. Statistical differences of the filamentous pattern (black bars) with respect to the wild-type distribution are indicated by asterisks (*$P<0.05$; **$P<0.01$).

effects shown by this latter are likely due to the presence of the p.E332K mutation rather than of the p.R330G mutation (Figure 1c).

Analysis of GFAP protein expression

As overexpression of the wild-type protein has been shown to induce aggregation in murine astrocytes *per se*,[7] and aggregation of mutant GFAP has been shown to induce inhibition of the proteasome activity with consequent raising in protein levels,[11] we have investigated whether the amount of aggregates in cells expressing the p.[R330G; E332K] GFAP could be associated with enhanced levels of the mutant protein.

First, we have assessed the involvement of the ubiquitin–proteasome system (UPS) in the degradation of mutant GFAP by observing both colocalization of ubiquitin in GFAP aggregates (Figure 2a) and a statistically significant increase in the percentage of cells containing a mutant GFAP exclusive aggregate pattern, consequent to treatment with the proteasome inhibitor lactacystin (Figure 2b). However, the comparison of mutant protein levels with the amount of wt GFAP has not shown any difference for the p.[R330G; E332K] mutant protein, while, as expected on the basis of the previous observations,[11] it has shown a significant increase for the p.R239C protein (Figure 2c).

Effects of the p.[R330G; E332K] mutant in wt GFAP and vimentin organization

As Alexander disease is characterized by a dominant inheritance, we have investigated whether the wild-type protein could be entrapped into aggregates containing the p.[R330G; E332K] GFAP mutant, thus accounting for dominant effects of the mutant protein. To this end, U251-MG cells were cotransfected with the p.[R330G; E332K]-GFP construct and a plasmid encoding the wild-type protein fused to a red fluorescent protein (HcRed). After checking that the proportion of cells characterized by a wild-type filamentous GFAP pattern was not altered by C-terminal fusion with the HcRed protein (data not

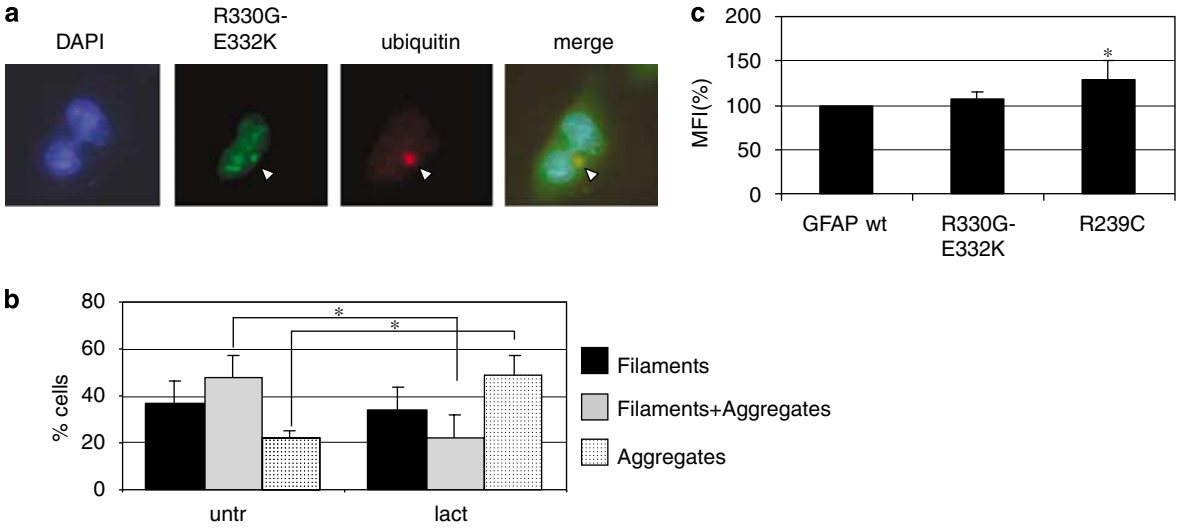

Figure 2 Analysis of the p.[R330G; E332K]-GFP GFAP protein accumulation in U251-MG cells. (**a**) Fluorescence microscopy images, showing colocalization of ubiquitin with an aggregate of the p.[R330G; E332K]-GFP protein. From left to right: DAPI stain of nuclei, green fluorescence of the GFP-fused mutant protein, red fluorescence of TRITC-conjugated ubiquitin-specific antibody, merge of the three images. (**b**) Diagram representation of the percentage of cells expressing the p.[R330G; E332K]-GFP protein characterized by the three GFAP patterns, with or without inhibition of the proteasome activity by lactacystin. (**c**) GFAP protein level, expressed as MFI, in U251-MG cells transfected with the wt-GFP (arbitrary value: 100), the p.[R330G; E332K]-GFP and p.R239C-GFP constructs. In any case, values are the mean ± SD of three independent experiments. Statistical differences with respect to the wild type are indicated by an asterisk (Student's *t*-test, $*P<0.05$). MFI, mean fluorescence intensity.

shown), morphological analysis in cells characterized by expression of both plasmids was performed. As shown in Figure 3a, in most cells green and red fluorescence showed colocalization. Moreover, in comparison with cells expressing only the wt GFAP-HcRed protein, coexpression of wt and p.[R330G; E332K]-GFP mutant caused a 30% decrease in cells presenting a wild-type filamentous structure (not shown), suggesting that the wt GFAP was entrapped into mutant protein inclusions, and therefore the occurrence of dominant effects of the mutant protein. Moreover, as GFAP can polymerize either on its own or with vimentin, we wondered whether the formation of GFAP aggregates due to forced expression of the mutant protein could disrupt the endogenous vimentin filamentous pattern. U251-MG cells, expressing endogenous vimentin, were stained with a TRITC-conjugated vimentin-specific antibody 48 h after transfection with the p.[R330G; E332K]-GFP expression construct. As reported in Figure 3b, two different GFAP–vimentin IF networks could be observed. In line I, a cytoskeletal pattern of p.[R330G; E332K]-GFP GFAP, characterized by numerous small aggregates placed on a filamentous network, is shown; in this case, observed in 80% cells, vimentin filaments display a normal spread organization without any dislocation or association with GFAP inclusions. On the other hand, line II shows a cell in which mutant GFAP organizes in a thick perinuclear pattern, disrupting the endogenous vimentin network by causing filaments to collapse around the nucleus; this latter was the rarest pattern among those observed, suggesting that disruption of IF cytoskeleton is not the main pathogenic mechanism of this mutation.

Rescue of wt GFAP phenotype consequent to KCl treatment

Recent studies have shown that the heat-shock protein αB-crystallin accumulates in Rosenthal fibers of patients with Alexander disease[18] and that its overexpression induces disaggregation of human GFAP inclusions.[8] Because of the low U251-MG cells transfection efficiency, to investigate the αB-crystallin effect on inclusions due to the p.[R330G; E332K] GFAP mutation, we decided to upregulate αB-crystallin indirectly, by the addition of KCl in the extracellular medium, rather than cotransfecting an αB-crystallin expression construct.[15,18] First, to confirm that our cellular system was responsive to KCl treatments, U251-MG cells were exposed to either 10 or 60 mM KCl for 24 h and analyzed for the αB-crystallin expression. As reported in Figure 4a, U251-MG cells show a marked dose-dependent increase in αB-crystallin transcript consequent to the addition of KCl in the culture medium, while untreated cells have undetectable levels of αB-crystallin expression. U251-MG cells were thus transfected with either the p.R239C or p.[R330G; E332K] GFAP mutant constructs and, the day after, added with 10 and 60 mM KCl. Twenty-four hours later, fluorescence analysis revealed that both KCl doses led the p.[R330G; E332K] GFAP mutant to organize a regular filamentous network in a very high percentage of cells (about 60%), suggesting a

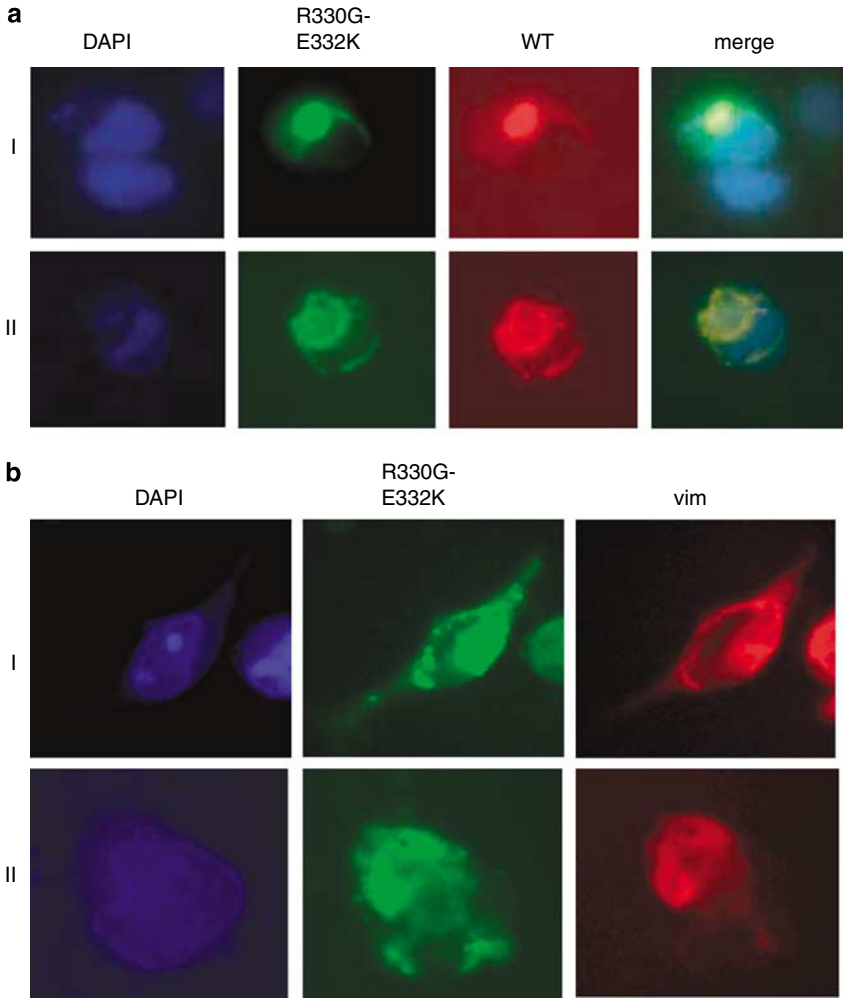

Figure 3 Cytoskeletal patterns induced by overexpression of the p.[R330G; E332K]-GFP mutant in U251-MG cells. (**a**) Microscope analysis of the localization of both wt GFAP and mutant GFAP in U251-MG cells. Two cells, expressing the p.[R330G; E332K]-GFP and the wt-HcRed GFAP fusion proteins and showing a pattern characterized by GFAP aggregates, are represented in the two rows (I and II). In particular, from left to right: nuclear DAPI staining (blue), GFP fluorescence (green, p.[R330G; E332K] mutant GFAP), HcRed fluorescence (red, wt GFAP), merge of the three images is shown for each cell. (**b**) Analysis of vimentin distribution in U251-MG cells expressing p.[R330G; E332K]-GFP. The three figures show DAPI staining of the nucleus (blue), GFAP expression (green) and vimentin staining (red), respectively, in a cell expressing the p.[R330G; E332K]-GFP GFAP mutation and characterized by a 'filaments + aggregates' pattern.

complete recovery of the wild-type phenotype in this cellular system (Figure 4b); although we observed a significant ability of p.R239C-transfected cells to rescue a filamentous pattern, the wild-type phenotype could not be achieved in this mutant. Finally, FACS analysis has shown no differences in mutant GFAP protein levels in cells grown with or without KCl treatment, thus excluding that our observations may be due to enhanced elimination of the misfolded protein (data not shown).

Discussion

In the present paper, we report a functional study aimed at elucidating the pathogenic effect of the co-occurrence of two mutations detected on a same *GFAP* allele, leading to p.[R330G; E332K], in four members of a family with recurrence of an adult form of Alexander disease.

To directly test the effect of the double amino-acid change, suggested by *in silico* analysis to induce protein conformational changes, cytoskeletal structures assembled by wt GFAP and mutant GFAP were visualized in transient transfections of human astrocytoma U251-MG cells. Overexpression of wt *GFAP* has been observed to induce development of cytoplasmic inclusions similar to Rosenthal fibers in mouse astrocytes[7] and formation of aggregated structures in several cellular models. Among these, the human astrocytoma U251-MG cells have been reported to show a very low proportion of wt

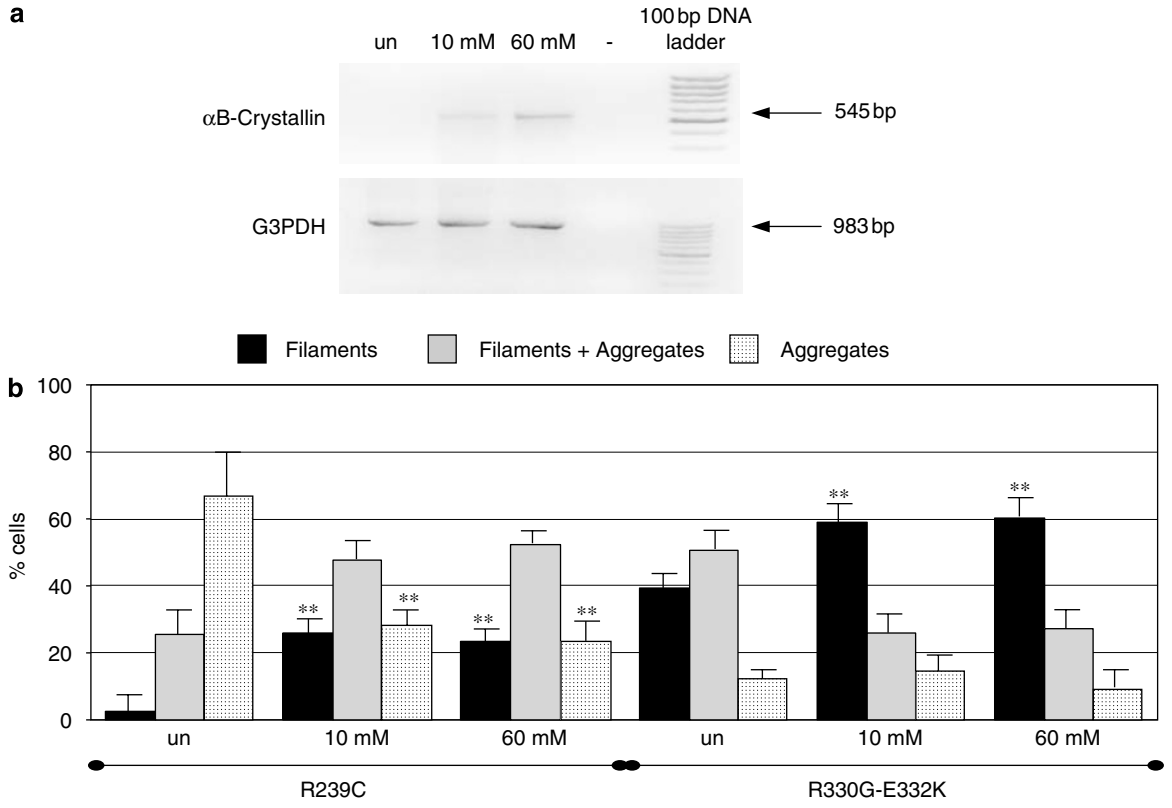

Figure 4 Effect of αB-crystallin on cytoskeletal organization of cells bearing mutant GFAP. (**a**) Induction of αB-crystallin expression in U251-MG cells. Upper panel: analysis of αB-crystallin mRNA in U251-MG cells cultured without any treatments ('un'), or in a medium containing 10 mM KCl ('10 mM') or 60 mM KCl ('60 mM'). Lower panel: housekeeping G3PDH mRNA in U251-MG cells under the same conditions. (**b**) Distribution of the three GFAP patterns in U251-MG cells transfected with the p.R239C-GFP and the p.[R330G; E332K]-GFP mutant proteins, following overexpression of αB-crystallin mRNA. Values are the mean ± SD of four independent experiments. Significant statistical differences between treated and untreated cells are represented with asterisks (Student's-*t*-test, $*P<0.05$; $**P<0.01$).

GFAP-transfected cells containing inclusions,[8,11] thus suggesting that they might be used as a suitable cell model to test our hypothesis.

Transient transfections in U251-MG cells have shown that cells characterized by aggregation of the p.[R330G; E332K] protein are significantly fewer than those containing p.R239C-induced aggregates. In addition, transfections of the single mutant proteins have suggested that the p.R330G alone does not have any effect, while the p.E332K seems to induce an uncorrected GFAP pattern in a significant fraction of cells, likely reflecting a major role played by this latter change in the complex allele-associated pathogenesis.

Moreover, the recent identification of the p.E332K substitution in another Italian patient affected with the adult-onset form of Alexander disease has confirmed the pathogenic role of this mutation when acting alone (DP, manuscript in preparation). In particular, this 61-year-old patient had a 4-year history of progressive limb weakness, followed by dysphonia due to vocal cord palsy and dysphagia. On examination, he also showed nystagmus, mild ataxia, pyramidal signs, and limb girdle wasting and weakness. Brain and cervical spinal cord radiological findings were consistent with those previously described in adult-onset Alexander disease with *GFAP* mutations.[19] Therefore, clinical observation and experimental results suggest to exclude a synergistic as well as a complementation effect of the two mutations within the complex allele, suggesting in addition that the p.E332K, and not the p.R330G, does contribute to the observed effects.

Recently, a positive feedback loop between GFAP accumulation and proteasome activity inhibition, mediated by activation of the MLK–JNK pathway, has been shown to sustain GFAP protein accumulation and aggregation.[11] We have confirmed the involvement of the UPS in the cell response to the p.[R330G; E332K] GFAP mutation. However, differently from what observed for the p.R239C mutant, FACS analysis did not show any significant increase of the p.[R330G; E332K] protein levels, thus excluding the accumulation of the mutant protein dependent on the complex allele as the main pathogenic effect and suggesting that further factors could play a role in the onset of this adult form of Alexander disease.

The interference of the mutant protein with wild-type correct polymerization, suggested by the observed drastic decrease of cells presenting a wt GFAP filamentous pattern in the presence of the p.[R330G; E332K] mutant protein, may be considered as an additional disease-causing mechanism induced by our mutation. This is in accordance with the reduced amount of cells presenting a GFAP regular pattern consequent to coexpression of wt GFAP and p.R239C mutant GFAP in SW13vim– cells,[10] and also with results obtained by (1) *in vitro* assembly assays showing that normal filaments are disrupted in the presence of the GFAP mutant p.R416W[17] and (2) colocalization of wt GFAP in aggregates containing the p.R239C mutant in astrocytoma cells.[11]

However, the very few interference of the p.[R330G; E332K] mutant in vimentin filaments organization is a further evidence that this *GFAP* mutation is not so deleterious.

We then wondered whether and how much *αB-crystallin* overexpression could induce the rescue of the filamentous pattern in cells expressing either the mild p.[R330G; E332K] or the severe p.239C alleles, a circumstance likely to further account for the differences observed in the disease severity associated with the two mutations. KCl has been used to induce *αB-crystallin* overexpression, although we cannot exclude additional effects of such a treatment on neurofilament organization and/or aggregate formation. In any case, treatment of cells with 10 mM KCl was sufficient to have a complete rescue of the correct GFAP filamentous phenotype in cells expressing the mild mutant, while a correct filamentous pattern was not completely achieved in cells expressing the severe allele at any KCl dose tested. The inefficacy in preventing aggregate formation observed by coexpressing *αB-crystallin* and murine p.R236H GFAP[20] does not seem in accordance with results obtained by us for the mild mutant. However, we believe that the partial rescue we achieved with the p.R239C mutant, equivalent to the murine p.R236H, can be explained by results observed by Mignot *et al*,[20] thus suggesting that severe GFAP mutations are more refractory than mild mutations to the cellular refolding mechanisms.

All these *in vitro* observations have shown less severe effects for the adult-onset-associated mutation in comparison with those observed for the p.R239C mutant, thus accounting for the different clinical and MRI features observed in association with the different Alexander disease forms.

In silico analysis of residue conservation in IFs has shown that the E332 residues lies within a sequence that shows a low degree of homology with other type III IFs. In particular, the observation that the E332 residue is present only in desmin and nestin seems to account for the not deleterious effect induced by the substitution.

The hypothesis that the mild effect of the novel allele could be due to its peculiar location is strengthened by our recent identification of the p.E332K mutation in an isolated case of adult Alexander disease (unpublished data) and by a recent report of a family characterized by dominantly inherited asymptomatic Alexander disease due to the missense substitution p.L331P,[21] suggesting that genetic anomalies in this region are likely associated with a mild disease phenotype.

References

1 Alexander WS: Progressive fibrinoid degeneration of fibrillary astrocytes associated with mental retardation in hydrocephalic infant. *Brain* 1949; **72**: 373–381.
2 Russo LS, Aron A, Anderson PJ: Alexander's disease: a report and reappraisal. *Neurology* 1976; **26**: 607–614.
3 Head MW, Corbin E, Goldman JE: Overexpression and abnormal modification of the stress alpha B-crystallin and HSP27 in Alexander disease. *Am J Pathol* 1993; **143**: 1743–1753.
4 Li R, Johnson AB, Salomons G *et al*: Glial fibrillary acidic protein mutations in infantile, juvenile and adult forms of Alexander disease. *Ann Neurol* 2005; **57**: 310–325.
5 Brenner M, Johnson AB, Boespflug-Tangury O, Rodriguez D, Goldman J, Messing A: Mutations in GFAP, encoding glial fibrillary acidic protein, are associated with Alexander disease. *Nat Genet* 2001; **27**: 117–120.
6 Rodriguez D, Gauthier F, Bertini E *et al*: Infantile Alexander disease: spectrum of GFAP mutations and genotype–phenotype correlation. *Am J Hum Genet* 2001; **69**: 1134–1140.
7 Messing A, Head MW, Galles K, Galbreath EJ, Goldman JE, Brenner M: Fatal encephalopathy with astrocytes inclusions in GFAP transgenic mice. *Am J Pathol* 1998; **152**: 391–398.
8 Koyama Y, Goldman J: Formation of GFAP cytoplasmic inclusions in astrocytes and their disaggregation by αB-crystallin. *Am J Pathol* 1999; **154**: 1563–1572.
9 Eliasson C, Sahlgren C, Berthold CH *et al*: Intermediate filament protein partnership in astrocytes. *J Biol Chem* 1999; **34**: 23996–24006.
10 Hsiao VC, Tian R, Long H *et al*: Alexander-disease mutation of GFAP causes filament disorganization and decreased solubility of GFAP. *J Cell Sci* 2005; **118**: 2057–2065.
11 Tang G, Xu Z, Goldman JE: Synergistic effects of the SAPK/JNK & the proteasome pathways on GFAP accumulation in Alexander disease. *J Biol Chem* 2006; **281**: 38634–38643.
12 Yoshida T, Tomozawa Y, Arisato T, Okamoto Y, Hirano H, Masanori N: The functional alteration of mutant GFAP depends on the location of the domain: morphological and functional studies using astrocytoma-derived cells. *J Hum Genet* 2007; **52**: 362–369.
13 Balbi P, Seri M, Ceccherini I *et al*: Adult-onset Alexander disease. Report on a family. *J Neurol* 2007; e-pub ahead of print 21 November 2007.
14 Bachetti T, Bocca P, Borghini S *et al*: Geldanamycin promotes nuclear localisation and clearance of PHOX2B misfolded proteins containing polyalanine expansions. *Int J Biochem Cell Biol* 2007; **39**: 327–339.
15 Sadamitsu C, Nagano T, Fukumaki Y, Iwaki A: Heat shock factor 2 is involved in the upregulation of αB-crystallin by high extracellular potassium. *J Biochem* 2001; **129**: 813–820.
16 Cheng J, Randall AZ, Sweredoski MJ, Baldi P: SCRATCH: a protein structure and feature prediction server. *Nucleic Acid Res* 2005; **33**: 73–76.
17 Perng MD, Su M, Wen SF *et al*: The Alexander disease-causing glial fibrillary acidic protein mutant, R416W, accumulates into Rosenthal fibers by a pathway that involves filament aggregation and the association of αB-crystallin and HSP27. *Am J Hum Genet* 2006; **79**: 197–213.

18 Iwaki T, Iwaki A, Fukumaki Y, Tateishi J: αB-crystallin in C6 glioma cells supports their survival in elevated extracellular K+: implication of the protective role of αB-crystallin accumulation in reactive glia. *Brain Res* 1995; **673**: 47–52.
19 Romano S, Salvetti M, Ceccherini I, De Simone T, Savoiardo M: Brainstem signs with progressing atrophy of medulla oblongata and upper cervical spinal cord. *Lancet Neurol* 2007; **6**: 562–570.
20 Mignot C, Delarasse C, Escaich S *et al*: Dynamics of mutated GFAP aggregates revealed by real-time imaging of an astrocyte model of Alexander disease. *Exp Cell Res* 2007; **313**: 2766–2779.
21 Shiihara T, Sawaishi Y, Adachi M, Kato M, Hayasaka K: Asymptomatic hereditary Alexander's disease caused by a novel mutation in *GFAP*. *J Neurol Sci* 2004; **225**: 125–127.